Restored UBE2C expression in islets promotes β-cell regeneration in mice by ubiquitinating PER1

Hemin Jiang
Jiangsu Province Hospital and Nanjing Medical University First Affiliated Hospital
Shuai Zheng
Jiangsu Province Hospital and Nanjing Medical University First Affiliated Hospital
Yu Qian
Jiangsu Province Hospital and Nanjing Medical University First Affiliated Hospital
Yuncai Zhou
Jiangsu Province Hospital and Nanjing Medical University First Affiliated Hospital
Hao Dai
Jiangsu Province Hospital and Nanjing Medical University First Affiliated Hospital
Yucheng Liang
Jiangsu Province Hospital and Nanjing Medical University First Affiliated Hospital
Yunqiang He
Jiangsu Province Hospital and Nanjing Medical University First Affiliated Hospital
Rui Gao
Jiangsu Province Hospital and Nanjing Medical University First Affiliated Hospital
Hui Lv
Jiangsu Province Hospital and Nanjing Medical University First Affiliated Hospital
Jie Zhang
Jiangsu Province Hospital and Nanjing Medical University First Affiliated Hospital
Zhiqing Xia
Jiangsu Province Hospital and Nanjing Medical University First Affiliated Hospital
Wenxuan Bian
Jiangsu Province Hospital and Nanjing Medical University First Affiliated Hospital
Tao Yang
Jiangsu Province Hospital and Nanjing Medical University First Affiliated Hospital
Qi Fu (drfuqi@njmu.edu.cn)
The First Affiliated Hospital of Nanjing Medical University https://orcid.org/0000-0002-2463-3123

Research Article

Keywords: UBE2C, β-cell regeneration, ubiquitination, PER1

Posted Date: January 24th, 2023

DOI: https://doi.org/10.21203/rs.3.rs-2483130/v1

Version of Record: A version of this preprint was published at Cellular and Molecular Life Sciences on July 24th, 2023. See the published version at https://doi.org/10.1007/s00018-023-04868-8.

Abstract

Background

The limited proliferation capacity of β-cells contributes to insulin insufficiency, which promotes the onset of diabetes. β-cells secrete multiple beneficial substances, except for insulin; therefore, the regeneration mechanism of β-cells requires further study. Previously, ubiquitin-binding enzyme 2C (UBE2C) was reported to be downstream of the key β-cell transcription factor NKX6.1, but the specific function and mechanism of UBE2C in pancreatic islets remain unknown.

Methods

We performed islet perfusion, immunofluorescence staining, and transmission electron microscopy (TEM) to examine the role of UBE2C in mice with a Cre-loxP-constructed β-cell-specific knockout (β*Ube2c*KO) or overexpression through lentivirus infusion within the pancreatic ducts. Single-cell RNA sequencing (scRNA-seq) and bulk RNA-seq, tandem mass tag (TMT) quantification proteomics, immunoprecipitation, and immunoblotting were conducted to explore the mechanisms by which UBE2C regulates β-cell proliferation.

Results

We discovered that ubiquitin-conjugating enzyme E2C (UBE2C) was highly expressed in a β-cell subgroup, which exhibited active proliferation capacity. We confirmed that UBE2C promotes β-cell compensatory proliferation by activating cell cycle renewal during a high-fat diet (HFD) and weaning. Consequently, β-cell-specific *Ube2c* knockout (β*Ube2c*KO) mice developed typical type 2 diabetes owing to β-cell loss caused by insulin insufficiency. Mechanistically, UBE2C combines with CUL1 to regulate PER1 degradation through ubiquitination. Notably, restored *Ube2c* expression in islets activated β-cell regeneration in streptozotocin (STZ)-induced diabetic mice, and alleviated diabetic hyperglycaemia and glucose intolerance.

Conclusion

This study indicates that UBE2C positively regulates β-cell proliferation by promoting ubiquitination and degradation of the biological clock suppressor PER1. The UBE2C-mediated beneficial effects on β-cells suggest a promising application in the treatment of diabetic patients with β-cell deficiency.

1. Introduction

Diabetes is characterised by hyperglycaemia caused by relative or absolute insulin [1, 2]. As a unique source of insulin, islet β-cells are either insufficient or lost [3–5]. However, kidney function protective C-

peptide [6, 7] and hepatic glucose output inhibitory non-coding RNA also originate from β-cells [8, 9], indicating an important role of β-cells in preventing diabetes progression. Therefore, protecting and promoting β-cell regeneration is more beneficial than traditional treatments such as insulin injection.

A lineage-tracing assay using β-cell-specific fluorescent mice showed that replication is the primary mode of β-cell regeneration [10]. Islet β-cells proliferate explosively during infancy and early childhood but decline gradually in conjunction with insulin secretory functional maturation. However, certain pathophysiological conditions, including obesity and pregnancy, can reactivate β-cell proliferation [11–13]. A major cause of type 2 diabetes is a poor diet, especially a high-fat load, which causes high numbers of individuals to develop the disease [14, 15]. Based on reports, type 2 diabetes only develops in patients who are unable to sustain β-cell compensation, and β-cell proliferative capacity loss is the main reason for this [16]. Exploring the mechanism of β-cell compensatory replication would provide key insights into β-cell regeneration and treatment of type 2 diabetes.

Owing to the different spatial distribution and maturity, significant heterogeneity of β-cells exists in the islets [17]. In the present study, single-cell RNA sequencing (scRNA-seq) was introduced to investigate subgroups of the same cell type, and scRNA-seq was then performed on high-fat diet (HFD)-induced obese mouse islets. A β-cell subgroup with explosive replication capacity was identified, and ubiquitin-binding enzyme 2C (UBE2C) was a top 3 characteristic gene of this group of cells. UBE2C is an important member of the E2 family, and its overexpression promotes proliferation and inhibits apoptosis of tumour cells [18, 19]. The E2 enzyme play a crucial “bridging” role in ubiquitin-labelling of target proteins, and its regulatory role in β-cell is not thoroughly understood. Although UBE2C has been reported to be downstream of the key β-cell transcription factor NKX6.1, which regulates β-cell proliferation [20], the specific function and mechanism of UBE2C in pancreatic islets remain unknown.

To investigate the regulatory mechanism of UBE2C to β-cell replication, β-cell-specific UBE2C conditional knockout (β*Ube2c*KO) mice were generated. β*Ube2c*KO mice developed hyperglycaemia due to β-cell loss-induced insulin insufficiency. Using immunoprecipitation and mass spectrometry (MS), the core protein of the SCF E3 ubiquitin-ligase complex, CUL1, was confirmed in combination with UBE2C. Moreover, the negative regulator of “biological clock” PER1 was investigated as the target of UBE2C/CUL1 complex. The degradation of PER1 then activates β cells through cell cycle initiation. Our investigation identified a previously unappreciated role of UBE2C in β-cell regeneration both *in vitro* and *in vivo* and supported the effectiveness of UBE2C restoration in the treatment of STZ-induced diabetic mice.

2. Materials And Methods

2.1. Animal experiments

Animal use procedures were approved (IACUC1804001) by the Medicine Animal Care Committee of Nanjing Medical University. Experiments were conducted in accordance with relevant institutional guidelines and regulations.

C57BL/6J and UBE2C$^{fl/fl}$ mice were purchased from the Model Animal Research Center of Nanjing University. MIP-Cre mice were obtained from Jackson Laboratory. To produce β-cell-specific knockout mice, UBE2C$^{fl/fl}$ mice were hybridised with MIP-Cre mice. In this study, mice with INS1-specific deletion of UBE2C were defined as β*Ube2c*KO mice and UBE2C$^{fl/fl}$ mice were used as controls. The genotype of the mice was analysed through polymerase chain reaction (PCR) using mouse-tail genomic DNA, and western blotting (WB) was used for verification at the protein level (Supplementary Fig. 2). β*Ube2c*KO mice and male C57BL/6J mice were maintained at 22°C on a 12-h light-dark cycle with *ad libitum* access to a normal chow diet (CD, 13.5% fat; LabDiet 5001) or HFD (60% fat; Research Diets D12492). Body weights were monitored periodically.

2.2. Tests for glucose and insulin

Mice were subjected to an intraperitoneal glucose tolerance test (IPGTT) and insulin tolerance tests (ITT) using established protocols [21].

2.3. Virus infusion within pancreatic ducts

Mice were injected with pSLenti-SFH-EGFP-P2A-Puro-CMV-Ube2c-3xFLAG-WPRE (LV-UBE2C) or pSLenti-SFH-EGFP-P2A-Puro-CMV-MCS-3xFLAG-WPRE (Vector) (OBIO Technology). Viruses were infused at 6 μL/min within pancreatic ducts as described previously [22].

2.4. Islet isolation and hormone-secretion assay

Isolation and culture of islets, islet/β-cell-cell line glucose-stimulated insulin secretion (GSIS) assay, and islet perfusion were performed as previously described [21]. Levels of insulin (Mercodia), glucagon (Mercodia), and somatostatin (Phoenix Pharmaceuticals) were measured using enzyme-linked immunosorbent assay (ELISA) kits, according to the manufacturer's instructions.

2.5. Transmission electron microscopy (TEM)

Islets were fixed in 2.5% glutaraldehyde and 2.5% paraformaldehyde in cacodylate buffer (0.1 M, pH 7.4). The TEM methods of primary mouse islets has been previously described [21]. Mature insulin granules were quantified using grayscale threshold analyses. The immature and docked granules were counted manually. Granules located within 100 nm of the plasma membrane without signs of fusion were considered "docked".

2.6. Immunofluorescence staining

Pancreatic tissue was fixed in formalin, incubated in ethanol and xylene, and embedded in wax. It was sliced into 5-μm sections, dewaxed in xylene, and rehydrated using a graded series of alcohol solutions. The sections were subjected to antigen retrieval and blocked with serum. Sections were incubated with primary antibodies overnight in the dark at 4°C. The antibodies used in this study are listed in Supplementary Table 1. After rewarming to room temperature and washing, sections were incubated with secondary antibodies for 2 h in the dark at room temperature. Images were acquired using a fluorescence microscope (Zeiss).

2.7. Cell culture

The mouse β-cell line, MIN6, was donated by Professor Zhuoxian Meng (Zhejiang University Medical College). Cells were cultured in Dulbecco's modified Eagle's medium (DMEM; Invitrogen, Carlsbad, CA, USA) containing 15% foetal bovine serum (FBS; Gibco), HEPES (10 mmol/L), sodium pyruvate (1 mmol/L), penicillin (100 U/mL), streptavidin (100 μg/mL), and β-mercaptoethanol (50 μmol/L).

The mouse β-cell line, βTC-6, was purchased from the Cell Bank of the Chinese Academy of Sciences (Kunming, China) and cultured in DMEM containing 10% FBS, penicillin (100 U/mL), streptavidin (100 μg/mL), and β-mercaptoethanol (50 μmol/L).

The human embryonic kidney cell line, 293T, was purchased from the Cell Bank of the Chinese Academy of Sciences (Shanghai, China) and cultured in DMEM containing 10% FBS, penicillin (100 U/mL), and streptavidin (100 μg/mL).

2.8. Co-immunoprecipitation

The cells were lysed in lysis buffer. After centrifugation, 10% of the supernatant was used as input, and the remainder was immunoprecipitated with agarose A/G beads (Roche), immunoglobulin G (IgG, negative controls), or with antibodies for the target proteins overnight at 4°C. Pellets were washed thrice with wash buffer, resuspended in sodium dodecyl sulphate (SDS, 2× concentration), and subjected to western blotting (WB).

2.9. WB

Cell lysates were prepared using RIPA lysis buffer on ice. The protein concentration was measured using the bicinchoninic acid (BCA) Assay Kit (Beyotime). WB was performed using the indicated antibodies (Supplementary Table 2). Protein blots were visualised using SuperSignal West Pico Chemiluminescent Substrate (Pierce Biotechnology) in a ChemiDoc XRS + system (Bio-Rad Laboratories).

2.10. MS and tandem mass tag (TMT) quantification proteomics

MS was performed on the precipitated protein using co-immunoprecipitation with UBE2C antibody of βTC-6 cells transfected with lentivirus-UBE2C or empty vectors, as previously described [24]. Quantification proteomics was performed on the total extracted protein of βTC-6 cells transfected with lentivirus-UBE2C or empty vectors using the TMT strategy, as previously described [23].

2.11. siRNA and plasmid transfection

MIN6 or βTC-6 cells were seeded in six-well plates and 24-well plates and cultured until they reached 70% confluence. Transient transfection with siRNA or plasmids was done using Lipo3000 (Life Technologies, Carlsbad, CA, USA). The siRNA sequences are listed in Supplementary Table 3.

2.12. Quantitative real-time PCR (qRT-PCR)

qRT-PCR was performed with SYBR Green PCR Master Mix (Takara Biotechnology) and analysed using a real-time PCR system (Roche), as previously described [21]. The primer sequences used are listed in Supplementary Table 4.

2.13. Bulk RNA-seq

Islets for RNA-seq were collected from the β*Ube2c*KO and control mice. RNA-seq methods have been previously described [24]. Gene expression was quantified using RSEM 1.1.12 software, and normalised using the method of fragments per kilobase of exon model per million reads mapped (FPKM). DEseq2 (fold change ≥ 2 and $p_{adjusted}$ ≤0·05) was used to identify differentially expressed genes (DEGs) between the β*Ube2c*KO and control groups.

2.14. Single-cell (sc)RNA-seq and datasets analysis

Islet cells from HFD and CD mice were dispersed into single cells and subjected to scRNA-seq, and the reads were processed as previously described [25]. The data were scaled and principal component analysis (PCA) was based on the top 2000 high variable genes. The top 20 principles were used for t-distributed stochastic neighbour embedding (t-SNE) and uniform manifold approximation and projection (UMAP) construction [26]. Using the Louvain method, the unsupervised cell cluster result was based on the top 20 principal components acquired using PCA [27]. We assigned β-cell types according to the expression of the marker gene Ins1. For the sub-clustering of β-cells, we applied the same scaling, dimensionality reduction, and clustering procedures. We identified significant DEGs among the β-cell subpopulations using the Wilcoxon rank-sum test. The DEGs were subjected to Kyoto Encyclopedia of Genes and Genomes (KEGG) enrichment analysis.

2.15. Cell-proliferation assay

Cell viability was determined using the Cell Counting Kit (CCK)-8 assay (Beyotime). Percent cell proliferation was detected using the 5-ethynyl-2'-deoxyuridine (EdU) assay (RiboBio). The ratio of cells positive for EdU to cells positive for 4',6-diamidino-2-phenylindole-positive (DAPI) was used to denote the percentage of EdU-positive cells. The cell cycle was detected using propidium iodide (PI) staining (Millipore Sigma).

2.16. Statistical analyses

The immunostaining of mouse pancreas sections was analyzed using ImageJ (Fiji) software and the data for each group were obtained from at least 20 islets. Data comparisons between the two groups were performed using two-tailed *t*-tests or analysis of variance (ANOVA) with Tukey's test which corrects for multiple hypotheses. AUC was calculated by trapezoid analysis and was compared by t-test. Data are the mean ± SD. Statistical significance was set at $P < 0.05$. Graphs and statistical analyses were completed using GraphPad Prism 8.0 (GraphPad Software, San Diego, CA, USA).

3. Results

3.1. ScRNA-seq showed *Ube2c* highly expressed in proliferating β-cells in mouse and human islets

To explore the pivotal mechanism promoting β-cell proliferation, scRNA-seq was performed on islets of C57BL/6J mice fed a HFD for 8 weeks which was confirmed by the compensatory proliferation period[21]. A total of 14108 β-cells from HFD- and CD-fed mice were annotated based on predominant hormone gene expression (Ins1) and then clustered into nine clusters using UMAP according to our previous study [28] (Fig. 1A). The cell cycle distribution of β-cells was further analysed, showing that Cluster-7 β-cells were in the G2M phase, whereas the other subpopulations were in the G1 and S phases (Fig. 1B). We then analysed the marker genes of cluster-7: *Ube2c* showed the Top3 highest expression in this cluster and was barely expressed in the remaining subpopulations (Fig. 1C). Therefore, we defined cluster-7 as *Ube2c*^{high} β-cells, and the remainder were defined as *Ube2c*^{low} β-cells (Fig. 1D). Gene set enrichment analysis (GSEA) revealed that *Ube2c*^{high} β-cells were enriched significantly in “DNA replication”, “cell cycle”, and “ubiquitin-mediated proteolysis pathways” (Fig. 1F). Functional enrichment analyses using Gene Ontology (GO) revealed biological processes to be associated with “mitosis” and “chromosome segregation”, and molecular functions to be associated with “cell cycle-dependent serine/threonine kinase activity” (Fig. 1G).

Compared to the *Ube2c*^{low} subpopulation, genes related to cell proliferation and cell cycle, such as *Pcna*, *Mki67, Ccnb2*, and *Cdk1*, were highly expressed in *Ube2c*^{high} subpopulation. However, the expression of genes related to β-cell maturation, such as *Slc2a2*, *G6pc2*, *Ucn3*, *Chga*, and *Ero1lb*, was slightly reduced. However, no difference was observed in the expression of *Ins1* and *Ins2* (Fig. 1E and H). Other DEGs are presented in Supplementary Table 5. Immunostaining confirmed the scRNA-seq findings, as Ki67, UBE2C, and INS were co-stained in pancreatic sections, indicating that high expression of *Ube2c* is a strong sign of proliferative β-cells (Fig. 2A).

To determine *UBE2C* expression levels in human islets, we used a recently reported dataset from non-diabetic donors [29]. Based on their annotated beta cells, *UBE2C* was specifically expressed in a very small population of cells (cluster 48). We defined cluster-48 as *UBE2C*^{high} β-cells and the remainder as *UBE2C*^{low} β-cells (Supplementary Fig. 1A–C). Both GO and KEGG analyses suggested that *UBE2C*^{high} β-cells were highly enriched in cell cycle and biological processes related to ubiquitination and DNA replication (Supplementary Fig. 1D–E). The cell proliferation-related genes *MKI67*, *CCNB2*, *CDK1*, *PCNA*, and *PBK*, and E3 ubiquitin ligase *CUL1* were highly expressed in *UBE2C*^{high} β-cells (Supplementary Fig. 1F). Other DEGs are presented in Supplementary Table 6. Moreover, a higher proportion of UBE2C positive β-cells was observed in human islets from an obese donor (BMI = 29.7) than in lean donors (BMI < 24) (Supplementary Fig. 1G). These results suggest that, similar to mice, UBE2C is also highly expressed in proliferating human β-cells.

3.2. Ube2c is highly expressed in islets of weaning and HFD-fed mice, and promotes β-cell proliferation

As previously reported, β-cells proliferate significantly physiologically during weaning and pathologically during the overnutrition-induced compensatory proliferation stage. The protein and RNA levels of islets were further investigated in CD and HFD-fed mice of various ages. In accordance with the RNA levels, WB analyses showed that UBE2C was highly expressed in juvenile mouse islets and increased when HFD was administered (Fig. 2B–D). This phenomenon was confirmed using immunohistochemical staining (Fig. 2E). However, the expression of UBE2C decreased with age. Importantly, these data were consistent with the decreased Ki67-positive β-cell ratio in mice fed an HFD in our previous study [21].

To determine whether *Ube2c* is the pivotal gene that regulates β-cell proliferation, gain- and loss-of-function were investigated in the mouse β-cell lines MIN6 and βTC-6. Increased cell viability and proliferation ratio were observed in the UBE2C over-expressing cell line; however, *Ube2c* knockdown diminished β-cell proliferation (Fig. 2F–M). As self-replication and expansion contribute to proliferation, PI staining combined with flow cytometry analysis was performed. We found a reduced proportion of cells in the G1 phase and an increased proportion of cells in the G2M phase in *Ube2c* knockdown βTC-6 cells compared to the control (Fig. 2N–O). Collectively, these data indicate that UBE2C promotes β-cell proliferation through self-replication based on cell cycle renewal.

3.3. β-cell specific Ube2c knockout impairs insulin secretion and glucose tolerance *in vivo*

To clarify the role of UBE2C in β-cells *in vivo*, β*Ube2c*KO mice were constructed (Supplementary Fig. 2A). Compared to wild-type (WT) mice, no significant difference in UBE2C expression was found in metabolic tissues of β*Ube2c*KO mice, such as liver, adipose tissue, and skeletal muscle, but expression was diminished in islets (Supplementary Fig. 2B–C). Physiologically, *Ube2c* knockout did not alter body weight (Fig. 3A) or fasting blood glucose levels but increased 2-h postprandial blood glucose levels in juvenile mice during 4-week-old weaning (Fig. 3B). Compared with control mice, β*Ube2c*KO mice developed glucose intolerance at 4 weeks of age and presented significantly higher plasma glucose levels during the glucose tolerance test (Fig. 3D). We further divided 4-week-old β*Ube2c*KO mice and their littermates randomly into HFD and CD groups to investigate the function of UBE2C during diabetic pathophysiology. Continuous monitoring of body weight showed increased body weight in HFD-fed mice compared with CD-fed mice; however, no significant difference was observed between β*Ube2c*KO and control mice (Fig. 3F). Mouse sex was also considered as a contributing factor for the metabolic phenotype, and no significant difference was found in body weight or blood glucose levels between β*Ube2c*KO and control female mice (data not shown); therefore, we selected male mice for subsequent studies. We found that the glucose clearance capacity of β*Ube2c*KO mice decreased significantly with prolonged HFD feeding compared to that of control mice (Fig. 3G–J).

To determine the main cause of decreased glucose clearance capacity, insulin and glucagon secretion, and insulin sensitivity of metabolic tissues were analysed. Compared to the control mice, β*Ube2c*KO mice showed impaired insulin secretion at 4 weeks old both in the fasting state or postprandially (Fig. 3C), and this phenomenon persisted in HFD feeding mice (Fig. 3L–M). However, glucagon secretion did not differ between β*Ube2c*KO and the control mice (Supplementary Fig. 4A–C). In addition, glucose-challenged insulin secretion was impaired in β*Ube2c*KO mice fed both CD and HFD (Fig. 3E and K). The ITT was used to estimate whole-body insulin sensitivity, and no difference was found between the control and β*Ube2c*KO mice (Supplementary Fig. 3A–C). We also assessed insulin sensitivity in the major insulin target organs; however, no significant change in the phosphorylated protein kinase B (p-AKT)/AKT ratio was found in β*Ube2c*KO mice compared to that in the control (Supplementary Fig. 3D–F). Collectively, these data suggest that *Ube2c* specific deletion in islet β-cells impairs insulin secretion, which contributes to hyperglycaemia in β*Ube2c*KO mice.

3.4. Decreased proliferation rate and secretory capacity of β-cells in β Ube2c KO mice result in impaired insulin secretion

To investigate the reasons for impaired insulin secretion in β*Ube2c*KO mice, pancreatic sections were used to analyse islet morphology. Based on the statistical analysis of hematoxylin and eosin (H&E) staining, a significant reduction in islet mass of β*Ube2c*KO mice compared to control mice had occurred by 4-week-old weaning (Fig. 4A). Moreover, islet size distribution analysis showed that the proportion of large islets decreased, but the proportion of small islets increased (Fig. 4B) in β*Ube2c*KO mice compared with control mice during CD feeding. The same tendency, but a more pronounced decrease in islet mass, was found after 4 weeks of HFD feeding in β*Ube2c*KO mice. Co-staining of insulin and glucagon was further performed to analyse whether β- or α-cell loss contributes to islet mass deficiency. Compared to the control mice, a smaller proportion of β-cells; however, a larger proportion of α cells in β*Ube2c*KO mice were noted (Fig. 4D). However, the comparatively high plasma glucagon levels in both fasting and postprandial states indicated that the relative increase in α-cell area was caused by β-cell reduction (Supplementary Fig. 4A–C). As described above, Ube2c was associated with β-cell replication, the proliferation indicators Ki67 and insulin were further co-stained, and a significantly decreased Ki67-positivite β-cell ratio was detected in β*Ube2c*KO mice both during off-lactation and in HFD feeding conditions (Fig. 4C and E). These data revealed that Ube2c knockout diminished the proliferative capacity of islet β-cells, resulting in inadequate amplification under metabolic stress, including nutrient changes from breastfeeding to carbohydrate or overnutrition.

Islet perfusion was performed on 4-week-old mice, and compared to the control mice, a significant decrease in glucose-stimulated second-phase insulin secretion was observed when corrected according to the DNA mass in β*Ube2c*KO mice (Fig. 4F). However, no difference was observed in the first phase of insulin secretion and insulin content. After 4 weeks of HFD feeding, the islet perfusion results of β*Ube2c*KO mice were similar to those of weaned mice, despite no statistical differences (Fig. 4G). *In vitro* GSIS experiments also showed that β*Ube2c*KO mice had significantly decreased insulin secretion in both CD and HFD feeding (Supplementary Fig. 4D and G). We further detected glucose-stimulated glucagon

and somatostatin secretion, and no significant difference was found between β*Ube2c*KO and control mice in either CD or HFD feeding (Supplementary Fig. 4D–I). Moreover, Ube2c overexpression in primary islets and βTC-6 cells improved GSIS when corrected based on protein levels (Supplementary Fig. 4J–L), whereas knockdown of UBE2C in βTC-6 cells decreased GSIS. These data indicated that UBE2C positively regulates insulin secretion, except for its ability to promote β-cell proliferation.

Considering the dampened glucose-stimulated insulin secretion of the Ube2c knockout, TEM was used to investigate the ultrastructure of β-cells, especially insulin granules. The total number of insulin granules decreased in β*Ube2c*KO mice at 4-week-old or after 4 weeks of HFD feeding (Fig. 4H). The reduction in mature insulin granules was the primary reason for total granule reduction, but not for immature or docked granules (Fig. 4I and J). Collectively, these data suggest that reduced β-cell mass contributes to the basal decrease in plasma insulin levels, whereas reduced mature granules contribute to glucose-stimulated insulin secretion *in vivo*, which finally promotes diabetes onset.

3.5. UBE2C promotes β-cell proliferation by ubiquitinating of PER1

Usually, UBE2C interacts with substrates and E3 ubiquitin ligases to ubiquitinate target proteins and degrade them through the proteasome pathway. The Cys114 site of human UBE2C protein is used to binds ubiquitin molecules. We found that human and mouse UBE2C were highly conserved; therefore, we constructed a mouse plasmid with the Cys mutation at the UBE2C114 site (UBE2C^{C114S}). The mouse cell line βTC-6 was transfected with WT, mutant (MT), and vector plasmids, and WB experiments revealed that UBE2CC114S did not affect UBE2C expression (Fig. 5A). Moreover, the CCK-8 and EdU assays showed that UBE2CC114S lost the capacity to promote β-cell proliferation compared to the WT plasmid (Fig. 5B–D), suggesting that the ubiquitin-binding site of UBE2C contributes to its molecular function.

To identify the possible substrate proteins and E3 binding to UBE2C, immune-precipitation and MS using the UBE2C antibody were performed. Using the immunoglobulin (Ig)G control, background proteins were removed, and 296 and 317 intercalating proteins were found in LV-GFP- (physiological condition) or LV-UBE2C- (proliferative condition) infected βTC-6 cells, respectively. In the physiological state, βTC-6 itself proliferates actively with high expression of UBE2C, and the high number of identified proteins (296) derived from the LV-GFP group reflects this condition. More interacting proteins (317) were identified after UBE2C overexpression, suggesting that the substrates of UBE2C in β-cells under physiological and proliferative conditions may differ. Among them, several core proteins in E3 ubiquitin ligase, including CUL1 (a member of the SCF complex), HERC2, CBLB, MID1, and members of the E1 ubiquitin activator UBA6, were detected (Fig. 5E). Quantification TMT proteomics of βTC-6 cell lines was also performed to identify possible target proteins that were expressed at lower levels after UBE2C overexpression (Fig. 5F). Venn diagrams showed that PER1 was the only protein detected in both the control and UBE2C-overexpression groups using the co-immunoprecipitation technique, and PER1 was decreased significantly after UBE2C overexpression (Fig. 5G). As ever reported that PER1 is an important negative regulator of “biological clock” that negatively regulates tumour proliferation, and the SCF complex can

degrade PER1 through ubiquitination [30, 31]. Besides, RNA-seq performed on HFD-fed control and β*Ube2c*KO mouse islets revealed that significant expressed genes enriched in “circadian entrainment pathway” (Fig. 5H–J), which corresponds to the function of the biological-clock gene Per1. Together, these data provide evidence that the UBE2C-CUL1-PER1 complex participates in β-cell proliferation.

We further proved that PER1 and CUL1 could co-precipitate using the UBE2C antibody (Fig. 6A), indicating that UBE2C interacts with PER1 and CUL1. The colocalisation of UBE2C and PER1 in islet β-cells was further verified by immunofluorescence (Fig. 6E). The transcriptional level of Per1 was detected using PCR, and we found that neither Ube2c overexpression nor knockout in primary islets influenced Per1 expression (Fig. 6F). However, WB showed that PER1 expression was reduced upon UBE2C overexpression, but increased in β*Ube2c*KO mice (Fig. 6B). We questioned whether UBE2C regulates PER1 expression through ubiquitination. Thus, we transfected the UBE2C WT and UBE2CC114S plasmids into βTC-6 cells and found that the UBE2CC114S plasmid did not cause a change in PER1 expression (Fig. 6C). The protein synthesis inhibitor cycloheximide (CHX) and proteasome inhibitor MG132 were then applied, and PER1 degradation was found to be significantly inhibited by MG132 (Fig. 6D), similar to the effect of Ube2c knockdown (Fig. 6G). The ubiquitination of PER1 was then detected in UBE2C WT and UBE2CC114S plasmid overexpressing cells, and UBE2C WT, but not UBE2CC114S, mediated the notable increase in PER1 ubiquitination (Fig. 6H). Co-immunoprecipitation also showed that UBE2C knockdown significantly reduced PER1 ubiquitination (Fig. 6I). The regulatory role of UBE2C to PER1 in β-cell proliferation and insulin secretion was further confirmed. PER1 inhibition significantly rescued UBE2C knockout-induced growth inhibition, and insulin secretion was observed in βTC-6 cells (Fig. 6J–L). Collectively, these results indicate that UBE2C reduced PER1 expression through ubiquitin-mediated proteasomal degradation, which contributes to the proliferation and glucose-stimulation of β-cells.

3.6. Restored UBE2C expression promotes β-cell regeneration in streptozotocin (STZ)-induced diabetic mice

As UBE2C promotes β-cell proliferation, we treated STZ-induced diabetic mice with massive β-cell loss (Fig. 7A). Low doses of STZ were injected into 4-week-old C57BL/6J mice for 5 d, and hyperglycaemia was monitored 1 month before virus injection (Fig. 7E–F). Ube2c-overexpressing and control lentiviruses were injected into the pancreatic duct at 8-week-old. Two weeks post injection, the UBE2C restored mice began to show a decrease in blood glucose levels and an increase in insulin levels (Fig. 7G–J).

With decreasing glucose levels, the body weight of Ube2c restored mice increase gradually compared to that of the control mice (Fig. 7B). Glucose tolerance was also improved in Ube2c restored mice owing to the increased glucose-stimulated insulin secretion *in vivo* (Fig. 7C and D). However, glucagon levels were not different between the groups (Fig. 7K), suggesting a specific effect of UBE2C on β-cells.

The co-staining of GFP and insulin showed widely expressed lentiviruses in the pancreas and more pronounced enrichment in islets (Fig. 7L). Interestingly, co-staining of Ki67 and insulin showed an increased proliferation rate of β-cell from Ube2c restored mice (Fig. 7M), which improved the proportion

of β-cells to α-cells (Fig. 7N), and recovered islet mass terminally (Fig. 7O). These data indicate the molecular function of Ube2c in β-cell proliferation and show its application prospects in diabetic patients with β-cell loss.

4. Discussion

We identified a vigorously proliferating subtype of β-cells, the highly expressed ubiquitin-binding enzyme UBE2C, which binds to the ubiquitin ligase CUL1 and jointly recognises the target protein PER1 to activate β-cell replication. The increased UBE2C promotes PER1 degradation through the ubiquitinated proteasome degradation pathway; the blocked cell cycle then begins to renew. Our investigation extends the previous mechanistic study of the NKX6.1/UBE2C axis in β-cell replication. Our results supported that regenerated β-cells can secrete insulin adaptive to blood glucose fluctuations, suggesting a better treatment compared to insulin injection.

The proportion of β-cells with proliferation capacity is nearly 1% in both adult human and murine islets but increases significantly in infants or in the initial stage in adults with chronic fuel surfeit [10–12]. β-cells with vigorous proliferation capacity are typically considered to have a weaker GSIS function and a lower maturity [32, 33]. Our investigation using bioinformatics and genetically modified mice proved that Ube2c could be a signature gene of the proliferative subgroup. In addition, genes associated with β-cell function, such as *Slc2a2*, *G6pc2*, *Ucn3*, *Chga*, and *Ero1lb*, were found to be slightly decreased, but not ins1 or ins2, suggesting a relatively immature of these cells. However, β*Ube2c*KO mice showed impaired GSIS either *in vivo* or *ex vivo*, indicating the essential role of UBE2C in GSIS function maintenance. Although we did not reveal the detailed mechanism of impaired insulin secretion, a recent study showed that PBK kinase-inactivated mice had a significant decrease in insulin secretion, whereas Pbk was found to be highly co-expressed with Ube2c in the subgroup of vigorously proliferating β-cells identified by us, which supports the plausibility of this phenomenon in β*Ube2c*KO mice[34].

UBE2C has been reported to mostly bind to the APC/C complex to promote target protein degradation [35] ; however, more than 600 types of E3 ubiquitin ligases have been found [36], and the details downstream of NKX6.1/UBE2C are elusive. Using a co-immunoprecipitation assay, our present study confirmed several targets of UBE2C, except for the APC/C complex, among which the core subunit of the SCF complex CUL1 has been reported to participate in cell cycle regulation [37, 38].

The biological clock system regulates the circadian clock as well as the cell cycle system, leading to regular mitosis and rhythmic DNA replication physiologically [39–42]. In circadian clock regulation, PER1 and PER2 combine CRY1 and CRY2, respectively, to inhibit CLOCK-BMAL1 activation [43]. As a negative regulator of cell division, PER1 also interacts with the cell-cycle-checkpoint proteins ATM/ATR and CHK1/2 [30]. Our co-immunoprecipitation and MS analyses identified PER1 as a target of the UBE2C/CUL1 complex. Although the role of PER1 in β-cell proliferation has not been proven *in vivo*, β-cell-specific per2 knockout mice showed alleviated glucose tolerance, in contrast to bmal1 knockout mice

[44–46]. The β*Ube2c*KO mice we used indicated that highly expressed PER1 promotes glucose intolerance by inhibiting β-cell proliferation.

Along with limited replication capacity, inflammatory infiltration, increased apoptosis, and de-/trans-differentiation of β-cells contribute to β-cell loss in an STZ-induced diabetic mouse model [47]. Our study showed that UBE2C induced β-cell replication was efficient in β-cell restoration. In addition, anti-apoptotic effects were observed in UBE2C highly expressed tumour cells [19]. Therefore, the molecular function of UBE2C in β-cell restoration requires further investigation.

Despite the explored mechanism of UBE2C in β-cell replication, our study had some limitations. First, NKX6.1 was reported to be the up-regulator of *Ube2c* transcription, whereas NKX6.1 was highly expressed in β-cell lifelong but not UBE2C. We did not reveal the conditional regulator of UBE2C expression. Additionally, further studies should be performed to determine the specific molecular mechanisms of UBE2C knockout-induced decline in beta insulin secretion and their relationship with PBK.

In summary, we found that the conditional highly expressed gene "*Ube2c"* is a signature of vigorous replicating β-cells. UBE2C positively regulates β-cell proliferation by promoting ubiquitination and degradation of the biological clock suppressor PER1. The mechanism of UBE2C in β-cells was used to treat STZ-induced diabetes in mice. Generally, our findings can be extended to further trials in which conditionally upregulated or downregulated genes can be used to treat diabetes.

Declarations

Author contributions

Q.F. and T.Y. directed the study and were responsible for study design and overall project management. H.J., S.Z., Y.Q. and Y.Z. performed statistical analyses, participated in study design, drafted the manuscript. H.D., Y.L., Y.Z., Y.H., J.Z., Z.X. and R.G. analyzed the data. H.L., W.B., and K.X. contributed to conception, design and interpretation of this work. All authors approved the final manuscript.

Funding

This work was supported by the National Natural Science Foundation of China (81830023, 82070803 and 82100837).

Data availability

The scRNA-seq analysis datasets during the current study are available in the Gene Expression Omnibus (GEO) repository under the accession number GSE203376 (mouse) and GSE148073 (human). Other datasets are available from the corresponding author upon reasonable request.

Acknowledgments

The authors wish to thank all research staff in Department of Endocrinology of the First Affiliated Hospital of Nanjing Medical University who participated in this work. We would like to thank the Core Facility of the First Affiliated Hospital of Nanjing Medical University for its help in the experiment.

Conflict of interest

The authors declare no competing financial interests.

Ethics approval

Animal use procedures were approved (IACUC1804001) by the Medicine Animal Care Committee of Nanjing Medical University. Experiments were conducted in accordance with relevant institutional guidelines and regulations.

References

1. Sims EK, Carr ALJ, Oram RA, DiMeglio LA, Evans-Molina C (2021) 100 years of insulin: celebrating the past, present and future of diabetes therapy. Nat Med 27(7): 1154-1164. 10.1038/s41591-021-01418-2
2. Mathieu C, Martens PJ, Vangoitsenhoven R (2021) One hundred years of insulin therapy. Nat Rev Endocrinol 17(12): 715-725. 10.1038/s41574-021-00542-w
3. Eizirik DL, Pasquali L, Cnop M (2020) Pancreatic Î²-cells in type 1 and type 2 diabetes mellitus: different pathways to failure. Nat Rev Endocrinol 16(7): 349-362. 10.1038/s41574-020-0355-7
4. Hudish LI, Reusch JE, Sussel L (2019) Î² Cell dysfunction during progression of metabolic syndrome to type 2 diabetes. The Journal of clinical investigation 129(10): 4001-4008. 10.1172/jci129188
5. Halban PA, Polonsky KS, Bowden DW, et al. (2014) Î²-cell failure in type 2 diabetes: postulated mechanisms and prospects for prevention and treatment. Diabetes Care 37(6): 1751-1758. 10.2337/dc14-0396
6. SamnegÃ¥rd B, Jacobson SH, Jaremko G, Johansson BL, SjÃ¶quist M (2001) Effects of C-peptide on glomerular and renal size and renal function in diabetic rats. Kidney Int 60(4): 1258-1265. 10.1046/j.1523-1755.2001.00964.x
7. Al-Rasheed NM, Willars GB, Brunskill NJ (2006) C-peptide signals via Galpha i to protect against TNF-alpha-mediated apoptosis of opossum kidney proximal tubular cells. J Am Soc Nephrol 17(4): 986-995. 10.1681/asn.2005080797
8. Li J, Zhang Y, Ye Y, et al. (2021) Pancreatic Î² cells control glucose homeostasis via the secretion of exosomal miR-29 family. J Extracell Vesicles 10(3): e12055. 10.1002/jev2.12055
9. Poy MN, Hausser J, Trajkovski M, et al. (2009) miR-375 maintains normal pancreatic alpha- and beta-cell mass. Proc Natl Acad Sci U S A 106(14): 5813-5818. 10.1073/pnas.0810550106
10. Dor Y, Brown J, Martinez OI, Melton DA (2004) Adult pancreatic β-cells are formed by self-duplication rather than stem-cell differentiation. Nature 429(6987): p.41-46

11. Parsons JA, Brelje TC, Sorenson RL (1992) Adaptation of islets of Langerhans to pregnancy: increased islet cell proliferation and insulin secretion correlates with the onset of placental lactogen secretion. Endocrinology(3): 1459
12. G K, M L, Habich K, Oberholzer M, Heitz PU (1985) Islet pathology and the pathogenesis of type 1 and type 2 diabetes mellitus revisited. Surv Synth Pathol Res 4(2): 110-125
13. Sorenson RL, Brelje TC (1997) Adaptation of islets of Langerhans to pregnancy: beta-cell growth, enhanced insulin secretion and the role of lactogenic hormones. Horm Metab Res 29(6): 301-307. 10.1055/s-2007-979040
14. Hu FB, Manson JE, Stampfer MJ, et al. (2001) Diet, lifestyle, and the risk of type 2 diabetes mellitus in women. N Engl J Med 345(11): 790-797. 10.1056/NEJMoa010492
15. Stott NL, Marino JS (2020) High Fat Rodent Models of Type 2 Diabetes: From Rodent to Human. Nutrients 12(12). 10.3390/nu12123650
16. Hudish LI, Reusch J, Sussel L (2019) β Cell dysfunction during progression of metabolic syndrome to type 2 diabetes. Journal of Clinical Investigation 129(12)
17. Avrahami D, Klochendler A, Dor Y, Glaser B (2017) Beta cell heterogeneity: an evolving concept. Diabetologia 60(8): 1363-1369
18. Liu PF, Chen CF, Shu CW, et al. (2020) UBE2C is a Potential Biomarker for Tumorigenesis and Prognosis in Tongue Squamous Cell Carcinoma. Diagnostics (Basel) 10(9). 10.3390/diagnostics10090674
19. Chiang AJ, Li CJ, Tsui KH, Chang C, Sheu JC (2020) UBE2C Drives Human Cervical Cancer Progression and Is Positively Modulated by mTOR. Biomolecules 11(1): 37
20. Tessem JS, Moss LG, Chao LC, et al. (2014) Nkx6.1 regulates islet β-cell proliferation via Nr4a1 and Nr4a3 nuclear receptors. Proc Natl Acad Sci U S A 111(14): 5242-5247
21. Gao R, Fu Q, Jiang HM, et al. (2021) Temporal metabolic and transcriptomic characteristics crossing islets and liver reveal dynamic pathophysiology in diet-induced diabetes. iScience 24(4): 102265. 10.1016/j.isci.2021.102265
22. Xiao X, Guo P, Prasadan K, et al. (2014) Pancreatic cell tracing, lineage tagging and targeted genetic manipulations in multiple cell types using pancreatic ductal infusion of adeno-associated viral vectors and/or cell-tagging dyes. Nat Protoc 9(12): 2719-2724. 10.1038/nprot.2014.183
23. Pagala VR, High AA, Wang X, et al. (2015) Quantitative protein analysis by mass spectrometry. Methods in molecular biology (Clifton, NJ) 1278: 281-305. 10.1007/978-1-4939-2425-7_17
24. Gao R, Fu Q, Jiang HM, Shen M, Yang T (2020) Temporal Metabolic Characteristics and Transcriptomic Landscape of Islets and Liver Reveal Dynamic Pathophysiology and Interorgan Crosstalk in High-fat Diet-induced Diabetes.
25. Wu AR, Neff NF, Kalisky T, et al. (2014) Quantitative assessment of single-cell RNA-sequencing methods. Nat Methods 11(1): 41-46. 10.1038/nmeth.2694

26. Kobak D, Berens P (2019) The art of using t-SNE for single-cell transcriptomics. Nature communications 10(1): 5416. 10.1038/s41467-019-13056-x
27. Subelj L, Bajec M (2011) Unfolding communities in large complex networks: combining defensive and offensive label propagation for core extraction. Phys Rev E Stat Nonlin Soft Matter Phys 83(3 Pt 2): 036103. 10.1103/PhysRevE.83.036103
28. Fu Q, Jiang H, Qian Y, et al. (2022) Single-cell RNA sequencing combined with single-cell proteomics identifies the metabolic adaptation of islet cell subpopulations to high-fat diet in mice. Diabetologia
29. Fasolino M, Schwartz GW, Patil AR, et al. (2022) Single-cell multi-omics analysis of human pancreatic islets reveals novel cellular states in type 1 diabetes. Nat Metab 4(2): 284-299. 10.1038/s42255-022-00531-x
30. Gery S, Komatsu N, Baldjyan L, Yu A, Koeffler HP (2006) The Circadian Gene Per1 Plays an Important Role in Cell Growth and DNA Damage Control in Human Cancer Cells. Molecular Cell 22(3): 375-382
31. Shirogane T, Jin J, Ang XL, Harper JW (2005) SCFβ-TRCP Controls Clock-dependent Transcription via Casein Kinase 1-dependent Degradation of the Mammalian Period-1 (Per1) Proteinm. Jbiolchem 280(29): 26863
32. Klochendler A, Caspi I, Corem N, et al. (2016) The Genetic Program of Pancreatic β-Cell Replication In Vivo. Diabetes 65(7): 2081-2093
33. Ruijtenberg S, Sander VDH (2016) Coordinating cell proliferation and differentiation: Antagonism between cell cycle regulators and cell type-specific gene expression. Cell Cycle 15(2): 196-212
34. Ma J, Xing B, Cao Y, et al. (2021) Menin-regulated Pbk controls high fat diet-induced compensatory beta cell proliferation. EMBO molecular medicine 13(5): e13524. 10.15252/emmm.202013524
35. Ben-Eliezer I, Pomerantz Y, Galiani D, Nevo N, Dekel N (2015) Appropriate expression of Ube2C and Ube2S controls the progression of the first meiotic division. FASEB journal : official publication of the Federation of American Societies for Experimental Biology 29(11): 4670-4681. 10.1096/fj.15-274522
36. Ye Y, Rape M (2009) Building ubiquitin chains: E2 enzymes at work. Nature reviews Molecular cell biology 10(11): 755-764. 10.1038/nrm2780
37. Xie J, Jin Y, Wang G (2019) The role of SCF ubiquitin-ligase complex at the beginning of life. Reprod Biol Endocrinol 17(1): 101. 10.1186/s12958-019-0547-y
38. Shirogane T, Jin J, Ang XL, Harper JW (2005) SCFbeta-TRCP controls clock-dependent transcription via casein kinase 1-dependent degradation of the mammalian period-1 (Per1) protein. The Journal of biological chemistry 280(29): 26863-26872. 10.1074/jbc.M502862200
39. Reppert SM, Weaver DR (2001) Molecular analysis of mammalian circadian rhythms. Annual review of physiology 63(1): 647
40. Yagita, K. (2001) Molecular Mechanisms of the Biological Clock in Cultured Fibroblasts. Science 292(5515): 278-281
41. Farshadi E, van der Horst GTJ, Chaves I (2020) Molecular Links between the Circadian Clock and the Cell Cycle. Journal of molecular biology 432(12): 3515-3524. 10.1016/j.jmb.2020.04.003

42. Takahashi JS (2017) Transcriptional architecture of the mammalian circadian clock. Nat Rev Genet 18(3): 164-179. 10.1038/nrg.2016.150
43. Ko CH, Takahashi JS (2006) Molecular components of the mammalian circadian clock. Hum Mol Genet 15 Spec No 2: R271-277. 10.1093/hmg/ddl207
44. Marcheva B, Ramsey KM, Buhr ED, et al. (2010) Disruption of the clock components CLOCK and BMAL1 leads to hypoinsulinaemia and diabetes. Nature 466(7306): 627-631. 10.1038/nature09253
45. Zhao Y, Zhang Y, Zhou M, Wang S, Hua Z, Zhang J (2012) Loss of mPer2 increases plasma insulin levels by enhanced glucose-stimulated insulin secretion and impaired insulin clearance in mice. FEBS Lett 586(9): 1306-1311. 10.1016/j.febslet.2012.03.034
46. Rakshit K, Hsu TW, Matveyenko AV (2016) Bmal1 is required for beta cell compensatory expansion, survival and metabolic adaptation to diet-induced obesity in mice. Diabetologia 59(4): 734-743
47. Bathina S, Srinivas N, Das UN (2017) Streptozotocin produces oxidative stress, inflammation and decreases BDNF concentrations to induce apoptosis of RIN5F cells and type 2 diabetes mellitus in Wistar rats. Biochem Biophys Res Commun 486(2): 406-413. 10.1016/j.bbrc.2017.03.054

Figures

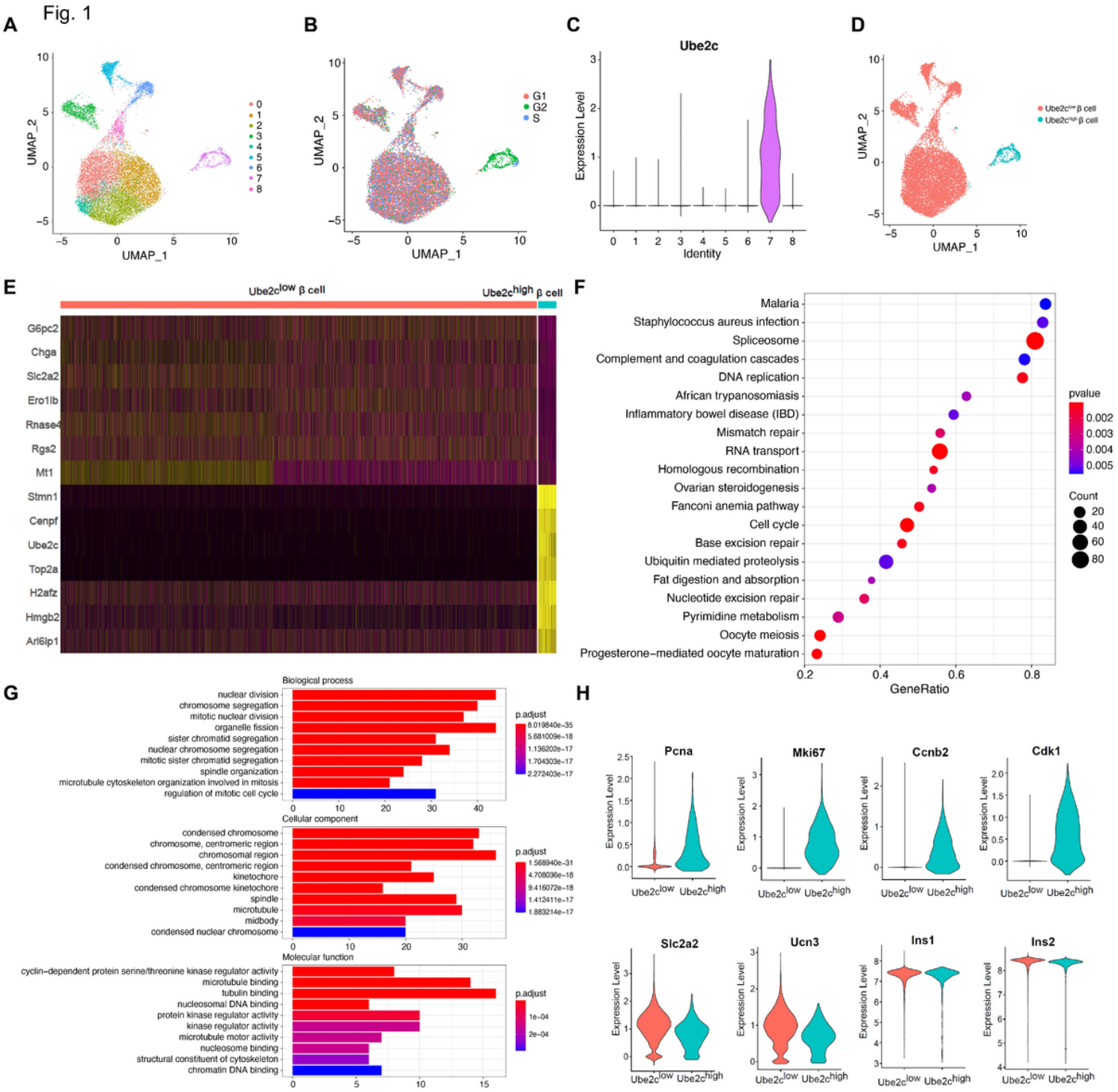

Figure 1

Heterogeneous expression of *Ube2c* on the islet β-cells of mice

(A) Visualization of β-cell clustering using uniform manifold approximation and projection (UMAP) maps;

(B) UMAP map showing cell-cycle distribution;

(C) Violin map showing *Ube2c* expression distribution in each β-cell subpopulation;

(D) UMAP map showing *Ube2c*^{high} and *Ube2c*^{low} subpopulations in β-cells.

(E) Heatmap of differentially expressed genes (DEGs) in *Ube2c*^{low} and *Ube2c*^{high} subgroups.

(F) GSEA pathway-enrichment map showing *Ube2c*^{high} β-cell subpopulations.

(G) DEGs between *Ube2c*^{high} and *Ube2c*^{low} subpopulation of β-cell based on the GO database.

(H) Violin plots of cell cycle- and β-cell function-related genes expressed in *Ube2c*^{low} and *Ube2c*^{high} subpopulations. Expression of *Pcna*, *Ki67*, *Ccnb2*, and *Cdk1* was upregulated markedly in *Ube2c*^{high} β-cells, expression of *Slc2a2* and *Ucn3* was upregulated slightly in *Ube2c*^{low} β-cells, and there was no difference in expression of *Ins1* or *Ins2*.

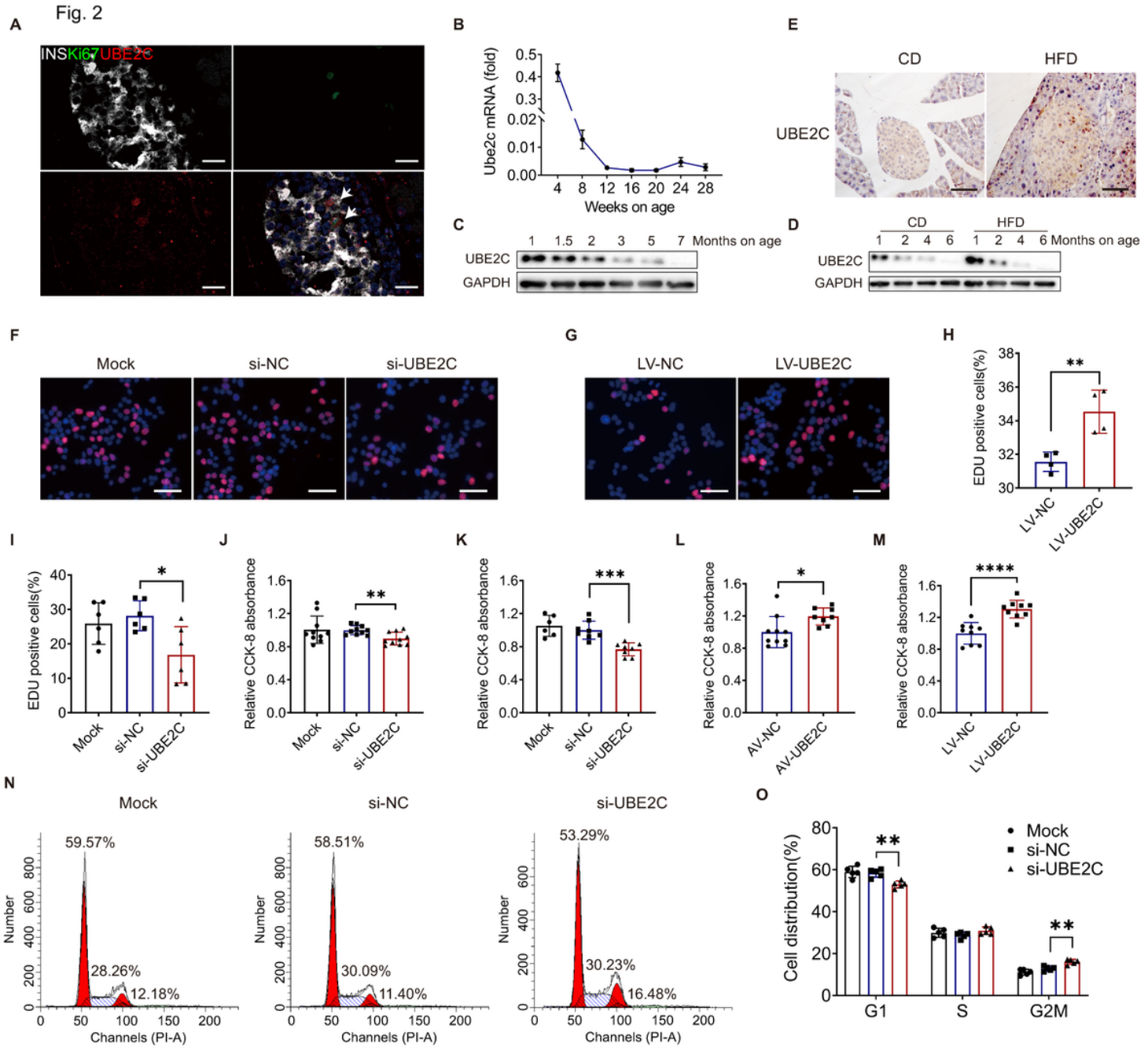

Figure 2

High expression of UBE2C promotes the proliferation of islet β-cells

(A) Representative images of insulin (white), Ki67 (green), UBE2C (red), and DAPI (blue) immunostaining in the pancreas of 4-week-old C57BL/6J mice. Scale bar: 20 μm.

(B and C) islets of chow-fed C57BL/6J mice 1, 1.5, 2, 3, 5, and 7 months after birth were extracted. (B) RT-qPCR formeasurement of expression of *Ube2c* mRNA, (C) western blotting to measure protein expression of UBE2C. (N=4-6mice/group)

(D) C57BL/6J male mice were fed with normal chow diet (CD) or high-fat diet (HFD) from 4 weeks of age, then islets were extracted at 1, 2, 4, and 6 months of feeding, and expression of UBE2C protein was measured in CD and HFD groups using western blotting. (N=3mice/group)

(E) Pancreatic sections of C57BL/6J mice after 4 weeks of HFD or CD feeding were assessed through immunohistochemistry using the UBE2C antibody. Scale bar: 40 μm.

(F and I) Cell proliferation was assessed using the EdU assay 72 h after si-UBE2C transfection of βTC-6 cells. (N=4 per group) Scale bar: 40 μm.

(G and H) Cell proliferation was assessed using the EdU assay 72 h after infection with UBE2C-overexpressing lentivirus (LV-UBE2C) of βTC-6 cells. (N=6 per group) Scale bar: 40 μm.

(J and K) Cell viability was assessed using the CCK-8 48 h after si-UBE2C transfection of MIN6 (J) and βTC-6 cells (K). (N=6-10 per group)

(L and M) Cell viability was assessed using the CCK-8 72 h after infection with UBE2C-overexpressing adenovirus (AV-UBE2C) in MIN6 (L) or lentivirus infection of βTC-6 cells (M). (N=6-10 per group)

(N and O) Representative images and proportional statistics of cell-cycle distribution using PI staining in βTC-6 cells after UBE2C knockdown. (N=5 per group)

*P<0.05, **P<0.01, ***P<0.001, ****P<0.0001.

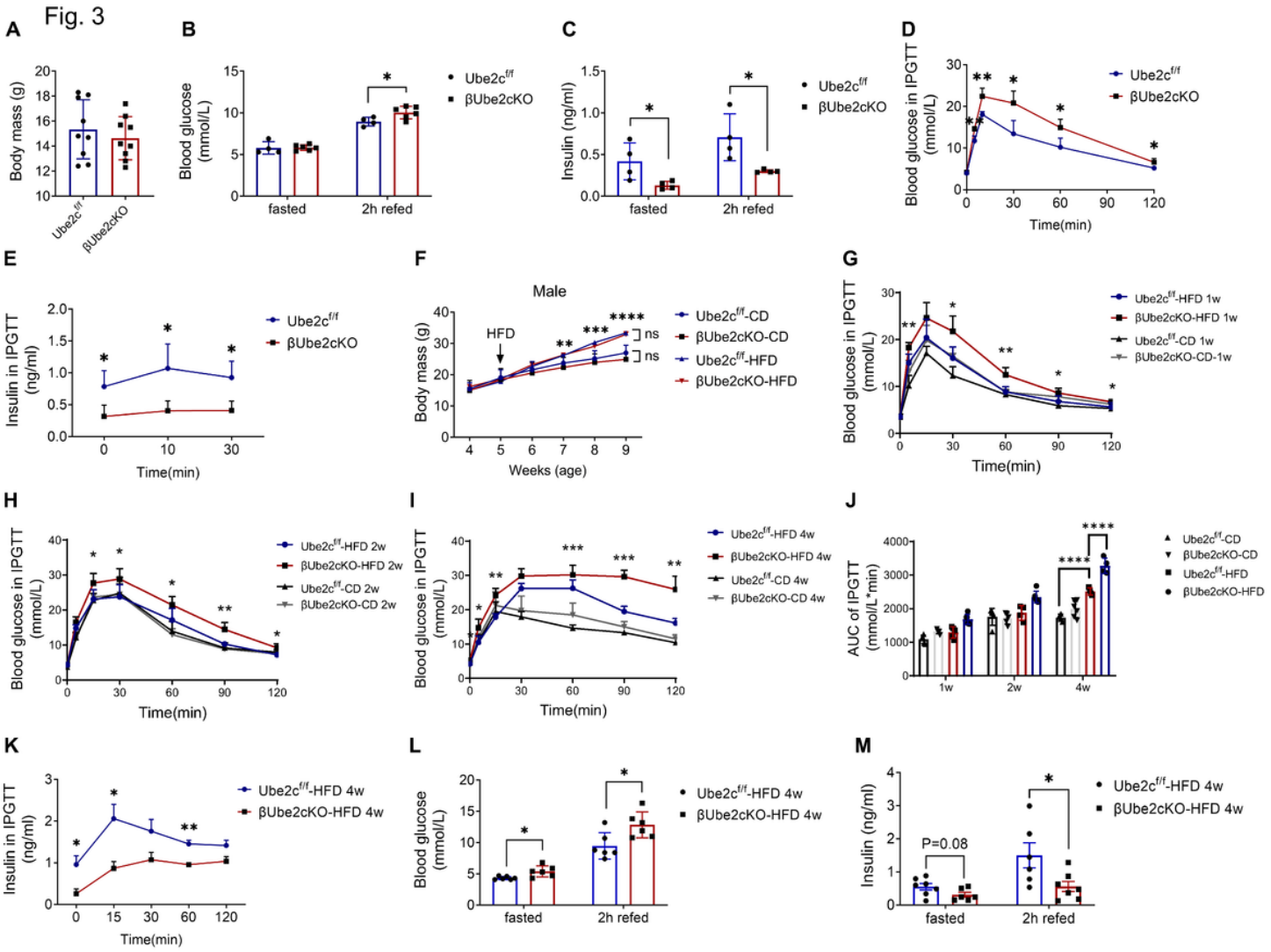

Figure 3

Impaired glycemic control in weaning and HFD-fed β*Ube2c*KO mice

(A) Bodyweights of 4-week-old β*Ube2c*KO weaning mice and littermate controls. (B and C) Fasting blood glucose and 2-h postprandial blood glucose (B), and fasting insulin and 2-h postprandial insulin (C) levels after a 12-h overnight fasting. (N = 4–10 mice/group)

(D and E) Intraperitoneal glucose tolerance on 4-week-old β*Ube2c*KO weaning mice: (D) Blood glucose level during IPGTT (2 g/kg glucose), (E) Plasma insulin concentration during the IPGTT (3 g/kg glucose). (N = 4–6 mice/group)

(F–M) The 4-week-old β*Ube2c*KO mice and controls were randomised into normal CD and HFD feeding groups after 1 week of adaptive feeding. (F) Weekly body weight measurements of the male mice. (G–I) Blood glucose levels at 0, 5, 15, 30, 60, 90, and 120 min under IPGTT (2 g/kg glucose) at 1, 2, and 4 weeks of CD or HFD feeding. (J) AUC calculation for glucose levels during the IPGTT. (K) Insulin levels at 0, 15, 30, 60, and 120 min during IPGTT in the HFD group after 4 weeks of feeding. (L, M) Fasting for 12 h after

4 weeks of HFD feeding, blood glucose and serum insulin levels of fasting and 2-h postprandial were measured.

N = 4–6 mice/group * P<0.05, ** P<0.01.

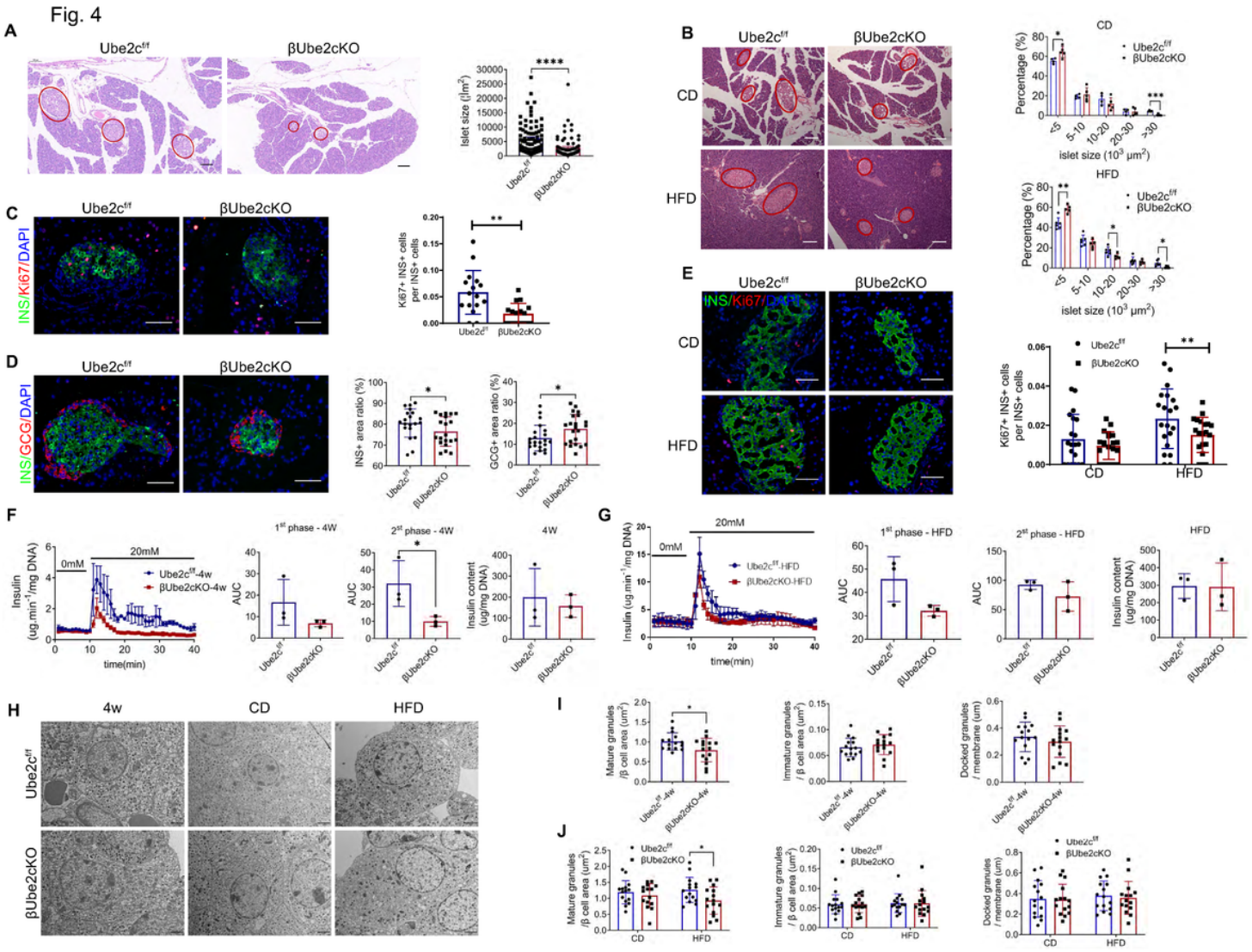

Figure 4

β*Ube2c*KO leads to the reduced proliferative and secretory capacity of islet β-cells to promote diabetes mellitus

(A and B) Representative H&E staining of pancreatic sections from β*Ube2c*KO and control mice at 4 weeks of age (A) or fed CD or HFD for 4 weeks (B) and size distribution of β-cells analysed by morphometry. (N=5 mice/group) Scale bar: 100 μm.

(C, E) Representative immunofluorescence images showing $Ki67^{+}$ INS^{+} cells in pancreatic sections from β*Ube2c*KO and control mice at 4 weeks of age (C) or fed CD or HFD for 4 weeks (E) (scale bar: 40 μm).

The percentage of $Ki67^+$ INS^+ cells in the total INS^+ cells is shown on the right. (N≥15 islets/group, N = 3–5 mice/group).

(D) Representative immunofluorescence images showing double-labelling for insulin (green) and glucagon (red) on pancreatic sections from β*Ube2c*KO and control mice at 4 weeks of age (scale bar: 40 μm). Quantification of insulin- and glucagon-stained areas is shown on the right side. (N=20 islets/group, N = 4–5 mice/group)

(F and G) Perfusion assays of islets were performed in β*Ube2c*KO mice of 4-week-old (F) and HFD feeding for 4 weeks (G). Islets were perfused with glucose (0 mM) for 0–10 min and high glucose (20 mM) for 10–40 min (N=120 islets/mouse, N = 3 mice per group). First-phase insulin secretion, second-phase insulin secretion, and intracellular insulin content are shown on the right side.

(H) Representative electron micrographs showing β-cells from β*Ube2c*KO and control mice at 4-week-old (F) or after 4 weeks of CD or HFD feeding (scale bar: 2 mm).

(I and J) Quantification of mature, immature, and docked insulin granules in β-cells of islets of β*Ube2c*KO and control mice at 4 weeks of age (I) and after 4 weeks of feeding with HFD or CD (J) (N = 12 β-cells/group, N = 6–8 islets/group, N = 3 mice/group).

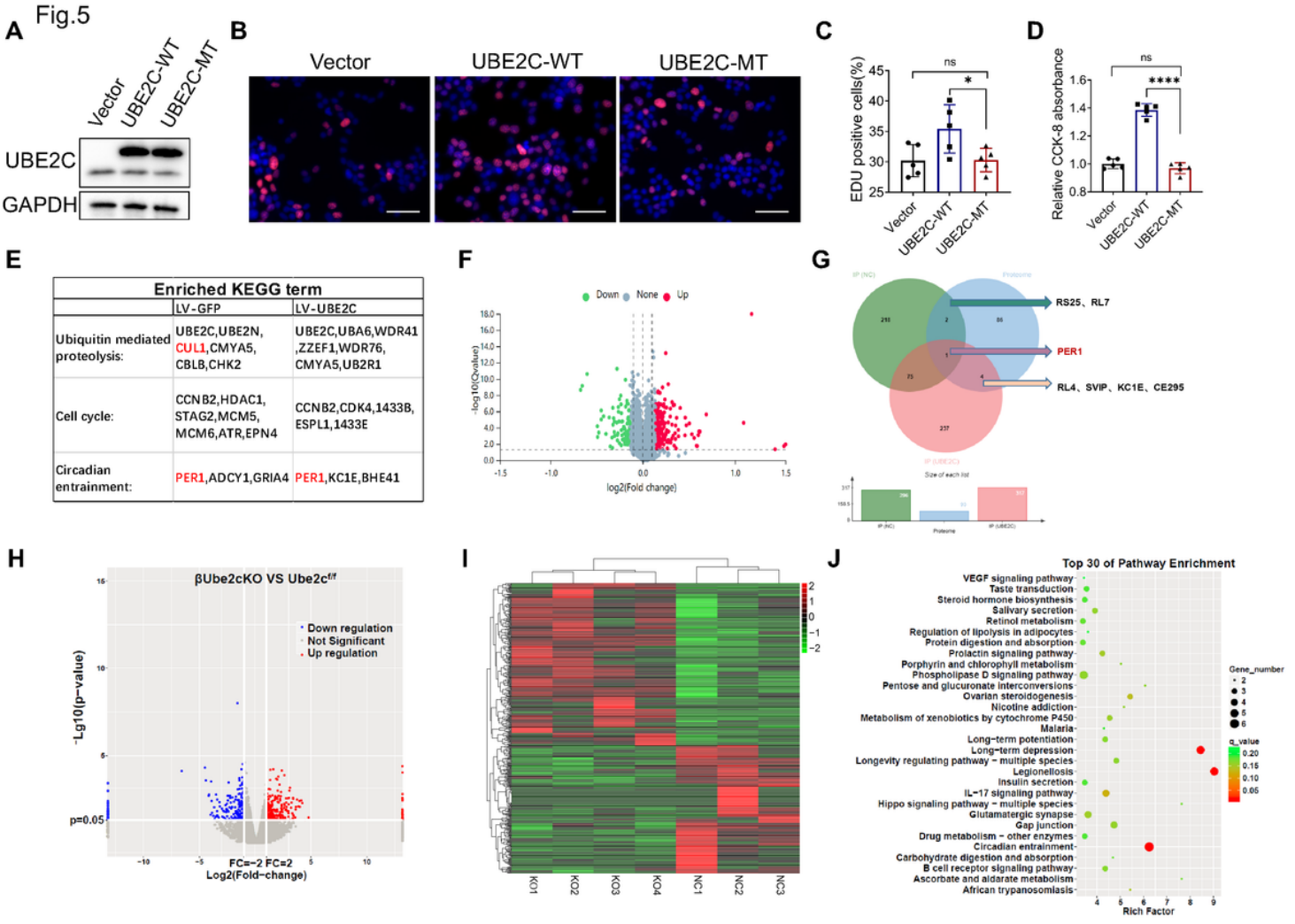

Figure 5

Co-immunoprecipitation combined with MS and RNA-seq for the target proteins of UBE2C ubiquitination

(A–D) The UBE2C ubiquitin-binding site mutant plasmid of mice ($UBE2C_{C114S}$) was constructed. The vector, WT, and MT plasmids were transfected with βTC-6 cells, (A) western blotting for UBE2C protein, (B and C) EdU for cell proliferation and (D) CCK-8 for cell viability. (N = 5 per group) *P<0.05, ****P<0.0001.

(E) An LV-UBE2C stably transformed βTC-6 cell line and the LV-GFP control strain were constructed. Total protein was extracted by MG132 (10 μmol/L) pretreatment for 4 h and analysed by co-immunoprecipitation and mass spectrometry with the UBE2C antibody. The KEGG database showed proteins to be enriched in “ubiquitination-mediated protein hydrolysis”, “cell cycle”, and” circadian entrainment” using mass spectrometry.

(F) Volcano plots of differentially expressed proteins (DEPs) for LV-UBE2C vs. the negative control (LV-NC) using TMT quantification proteomics. (G) Venn diagrams of protein analysis by CO-IP mass spectrometry and downregulated DEPs from TMT quantification proteomics (LV -UBE2C vs LV-NC).

(H–J) Extracted islets from HFD-fed β*Ube2c*KO and control mice at 4 weeks of age were subjected to RNA-seq, and DEGs were screened using |FC| > 2 and P < 0.05. (H and I) Volcano plots and heatmaps of DEGs. (J) Analysis of signalling-pathway enrichment of DEGs using the KEGG database.

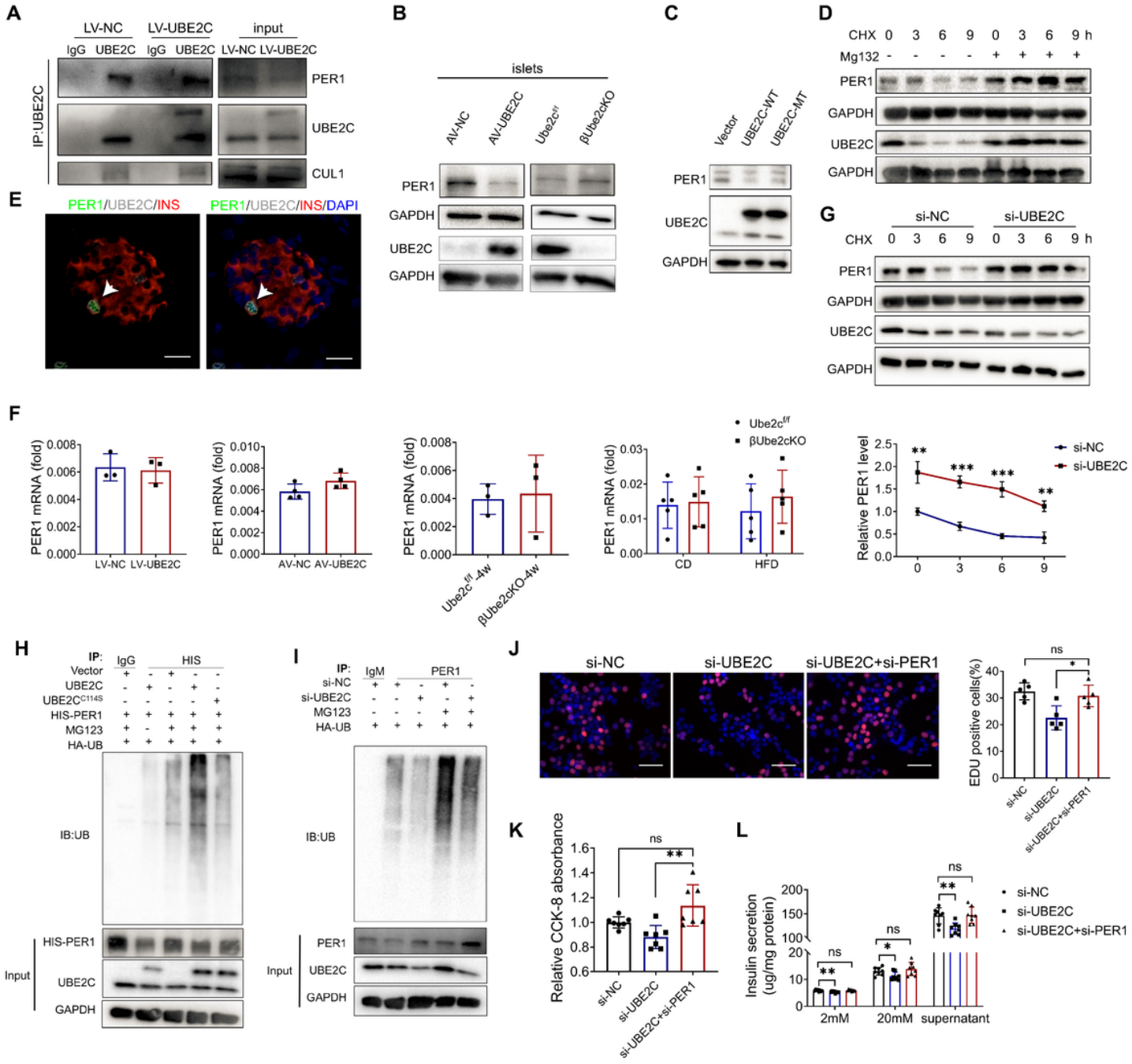

Figure 6

UBE2C regulates PER1 degradation by ubiquitination

(A) LV-UBE2C stably transfected βTC-6 cell line and control line were constructed. Pretreatment with MG132 (10 μmol/L) for 4 h was performed. Total protein was extracted for co-immunoprecipitation with UBE2C antibody. Protein expression of PER1, UBE2C, and CUL was measured using western blotting.

(B) Islets were overexpressed/knockout for UBE2C followed using western blotting detection of expression of PER1 protein.

(C) Western blotting detection of PER1-protein expression in βTC-6 cells transfected with null, wild type (WT), mutant (MT) plasmids.

(D) Western blotting detection of protein expression of PER1 and UBE2C in βTC-6 cells treated with CHX (50 μg/mL) with or without MG132 (10 μmol/L) for 0, 3, 6, and 9 h.

(E) Representative images of UBE2C (white), PER1 (green), INS (red), and DAPI (blue) immunostaining in the pancreas of 4-week-old C57BL/6J mice. Scale bar: 20 μm.

(F) *Per1* mRNA expression in βTC-6 and islets overexpressing UBE2C; *Per1* mRNA expression in β*Ube2c*KO mice at 4 weeks of age and fed with HFD for 4 weeks in islets. (N = 3–6 per group)

(G) After treatment of βTC-6 cells with si-UBE2C and treatment with CHX (50 μg/mL) for 0, 3, 6, and 9 h before sample collection, protein expression of PER1 and UBE2C was detected using western blotting and the rate of PER1 degradation was calculated. (N = 3)

(H) HA-UB, 6*HIS-PER1, and UBE2C null control or WT or MT-overexpression plasmids were co-transfected into HEK293T cells, treated with or without MG132 for 4 h before sample collection, and PER1 ubiquitination in each group was measured usingwestern blotting of a ubiquitin antibody after co-immunoprecipitation with HIS-tagged antibody.

(I) βTC-6 treated with si-UBE2C was transferred into HA-UB plasmids with or without MG132 treatment for 4 h before sample collection, and PER1 ubiquitination in each group was detected using western blotting of a ubiquitin antibody after co-immunoprecipitation with PER1 antibody.

(J–L) si-UBE2C and si-PER1 were co-transfected with βTC-6 cells. (J) EdU assay for cell proliferation in the si-NC, si-UBE2C, and si-UBE2C+si-PER1 groups (scale bar:40 μm); (K) CCK-8 assay for cell viability and (L) GSIS assay for insulin secretion. (N = 7-8 per group)

*P<0.05, **P<0.01, ***P<0.001, ****P<0.0001.

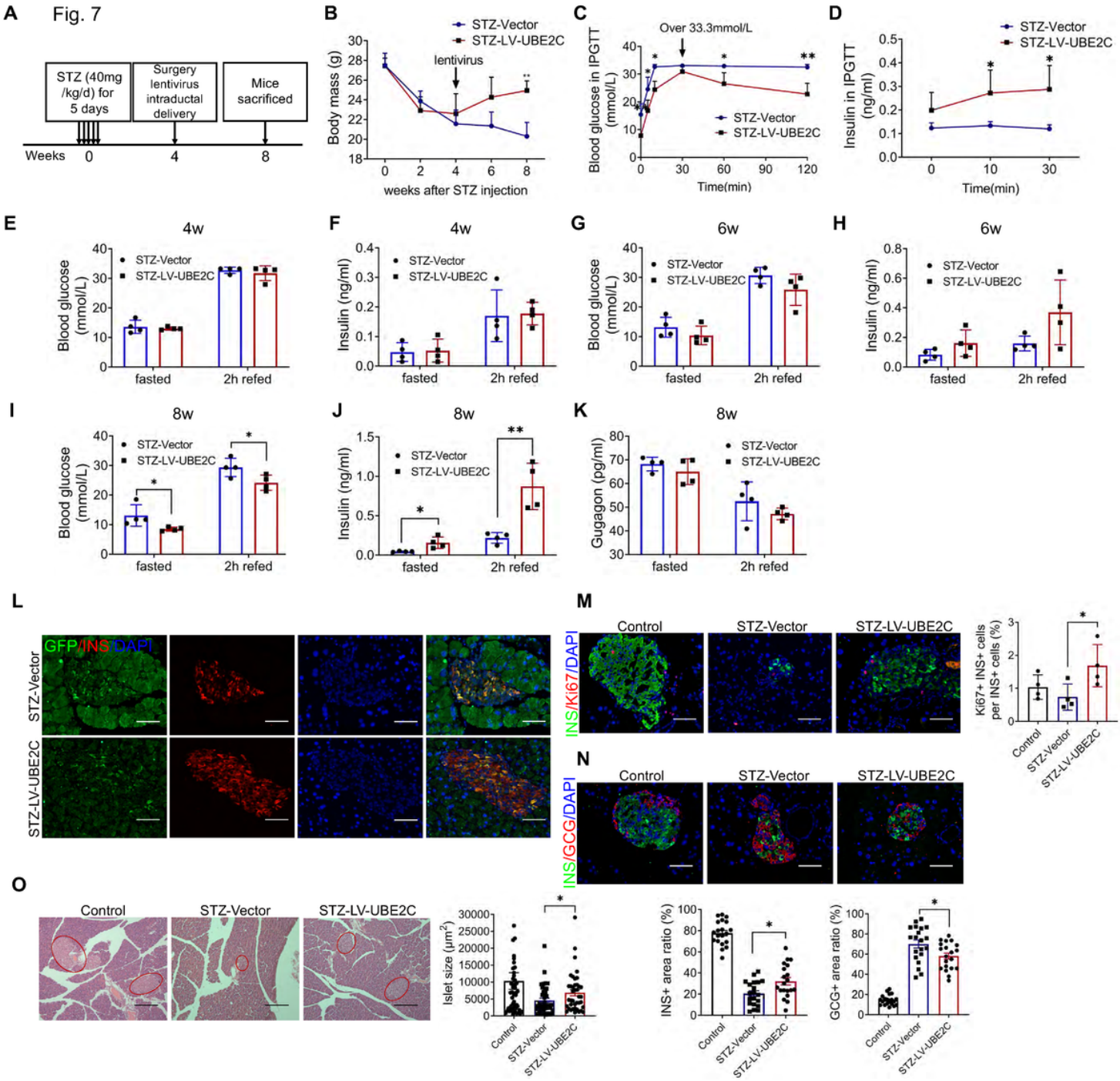

Figure 7

UBE2C promotes islet β-cell regeneration in STZ-induced DM mice

(A) Experimental procedure (schematic).

(B) Bodyweights of UBE2C-overexpressing and control mice were measured weekly after STZ injection. N = 4 mice/group

(C, D) IPGTT glucose- and insulin-release curves 4 weeks after *in situ* injection within pancreatic ducts. N = 4 mice/group

(E–J) Blood glucose and serum insulin levels before (E, F), 2 weeks (G, H), and 4 weeks (I, J) post-injection (corresponding to 4, 6, and 8 weeks after STZ modelling, respectively) fasting, and 2 h after resumption of feeding in the pancreatic ducts before *in situ* injection of UBE2C lentivirus. (K) Serum glucagon levels 4 weeks after *in situ* pancreatic duct injection, fasting, and 2 h after meal consumption; N = 4 mice/group, *P<0.05, **P<0.01.

(L) Immunofluorescence co-staining of GFP (green) and INS (red) in pancreatic sections after 4 weeks of treatment to observe pancreatic GFP expression (scale bar:40 μm).

(M) Representative images of immunofluorescent double-stained INS (green) and Ki67 (red) and statistical plots of Ki67 and INS double-positive cells as a percentage of total INS_+ cells in normal C57BL/6J mice, the STZ-Vector group, and the STZ-LV-UBE2C group based on H&E staining (scale bar: 40 μm). N≥20 islets/group, N = 4 mice/group, *P<0.05.

(N) Immunofluorescence double-stained INS (green) and GCG (red) islets and area values showing the percentage of insulin and glucagon positivity in islets (scale bar:40 μm); (O) Representative image of H&E staining (islets circled by red dashed lines) and the area of individual islets (scale bar:100 μm). N≥20 islets/group, N = 4 mice/group, *P<0.05.

Supplementary Files

This is a list of supplementary files associated with this preprint. Click to download.

- SupplementaryFigures.pdf
- SupplementaryTable14.docx
- SupplementaryTable5mouseUBE2ClowhighDEGs.xlsx
- SupplementaryTable6humanUBE2ClowhighDEGs.xlsx
- GraphicAbstract.pdf